Neuro-Oncology
XX(XX), 1–13, 2020 | doi:10.1093/neuonc/noaa206 | Advance Access date 2 September 2020

NEO100 enables brain delivery of blood–brain barrier impermeable therapeutics

Weijun Wang[†], Nagore I. Marín-Ramos,[†] Haiping He, Shan Zeng, Hee-Yeon Cho, Stephen D. Swenson, Long Zheng, Alan L. Epstein, Axel H. Schönthal, Florence M. Hofman, Ligang Chen, and Thomas C. Chen

Department of Neurological Surgery, USC, Luzhou, China (W.W., N.I.M-R., H.H., S.Z., H-Y.C., S.D.S., T.C.C.); Department of Neurosurgery, Affiliated Hospital of Southwest Medical University, Luzhou, China (H.H., S.Z., L.C.); Department of Pathology, Keck School of Medicine, University of Southern California (USC), Los Angeles, California, USA (L.Z., A.L.E., F.M.H.); Departments of Microbiology and Immunology, Keck School of Medicine, USC, Los Angeles, California, USA (A.H.S., T.C.C.)

[†]These authors contributed equally to this project.

Corresponding Author: Thomas C Chen, MD, PhD, Departments of Pathology and Neurosurgery, Keck School of Medicine, University of Southern California, 2011 Zonal Avenue, Los Angeles, CA 90033 (thomas.chen@medmail.usc.edu).
Co-Corresponding Author: Ligang Chen, MD, PhD, Department of Neurosurgery, Affiliated Hospital of Southwest Medical University, 25 Taiping Street, Jiangyang Region, Luzhou, P.R China 646000 (chengligang.cool@163.com).

Abstract

Background. Intracarotid injection of mannitol has been applied for decades to support brain entry of therapeutics that otherwise do not effectively cross the blood–brain barrier (BBB). However, the elaborate and high-risk nature of this procedure has kept its use restricted to well-equipped medical centers. We are developing a more straightforward approach to safely open the BBB, based on the intra-arterial (IA) injection of NEO100, a highly purified version of the natural monoterpene perillyl alcohol.

Methods. In vitro barrier permeability with NEO100 was evaluated by transepithelial/transendothelial electrical resistance and antibody diffusion assays. Its mechanism of action was studied by western blot, microarray analysis, and electron microscopy. In mouse models, we performed ultrasound-guided intracardiac administration of NEO100, followed by intravenous application of Evan's blue, methotrexate, checkpoint-inhibitory antibodies, or chimeric antigen receptor (CAR) T cells.

Results. NEO100 opened the BBB in a reversible and nontoxic fashion in vitro and in vivo. It enabled greatly increased brain entry of all tested therapeutics and was well tolerated by animals. Mechanistic studies revealed effects of NEO100 on different BBB transport pathways, along with translocation of tight junction proteins from the membrane to the cytoplasm in brain endothelial cells.

Conclusion. We envision that this procedure can be translated to patients in the form of transfemoral arterial catheterization and cannulation to the cerebral arteries, which represents a low-risk procedure commonly used in a variety of clinical settings. Combined with NEO100, it is expected to provide a safe, widely available approach to enhance brain entry of any therapeutic.

Key Points

1. IA NEO100 safely and reversibly opens the BBB in mouse models.
2. BBB opening by IA NEO100 enables effective brain entry of various-sized therapeutics.
3. Clinical use of IA NEO100 could have revolutionary impact on CNS drug delivery.

Importance of the Study

There is an urgent medical need to improve the transportation of therapeutics into the central nervous system (CNS), which is generally impeded by the BBB. Intra-arterial (IA) mannitol is currently used in clinical practice to deliver non-BBB-permeable therapeutics, but it represents an unreliable technique that leads to variable degrees of BBB disruption, with subsequent fluctuating concentrations of drugs in the cerebrospinal fluid. In comparison, NEO100 induces an immediate, efficient, reversible and safe BBB opening in mice. IA NEO100-mediated BBB permeabilization facilitates the brain distribution of non-BBB-permeable therapeutics of different sizes, including methotrexate, anti–programmed cell death 1 antibody and CAR T cells. IA NEO100 could cause a positive revolutionary impact on drug delivery of therapeutics to target brain malignancies and CNS disorders.

The blood–brain barrier (BBB) is a dynamic biologic interface that controls the exchange of substances between the blood and the central nervous system (CNS). The structural and functional integrity of the BBB is vital for the maintenance of homeostasis in the CNS.[1] However, it impedes the entry of drugs into the CNS, preventing many potent pharmaceutical agents from exerting substantial therapeutic activity against CNS disorders and brain-related malignancies.[1] Currently, BBB disruption via rapid intra-arterial (IA) infusion of hyperosmolar mannitol represents the main clinical method to obtain a transient BBB opening.[2] However, the fluctuations in BBB disruption obtained with mannitol can have a negative impact on the regional delivery of therapeutics, along with unpredictable adverse effects, such as seizures, risks of brain embolism, catastrophic bleeds, and even fatal brain edema.[3,4] Therefore, a novel approach to obtain a safe, controlled, transient BBB permeabilization effect is badly needed.

We had previously demonstrated that intranasal delivery of NEO100, a cyclic guanosine monophosphate–quality version of the natural monoterpene perillyl alcohol (POH), is effective for the treatment of temozolomide (TMZ)-resistant human glioma xenografts in an athymic nu/nu mouse model.[5] POH has been extensively tested both in the laboratory and in human patients showing promising results in glioma treatment.[6,7] NEO100 is currently being used in a phase I/II clinical trial for the treatment of recurrent glioblastoma.[8] It is generally accepted that intranasal delivery bypasses the BBB by using cranial nerve to brain transport (specifically, cranial nerves I and V). Given its physicochemical properties, we hypothesized that NEO100 could also have a direct effect on BBB integrity. Here, we study the effects on BBB disruption when NEO100 is given by IA application. Our preliminary data showed that IA NEO100, but not intravenous NEO100, induces an immediate, transient, and reversible opening of the BBB, allowing penetration into the brain parenchyma and cerebrospinal fluid (CSF) of non-BBB-permeable therapeutics, including methotrexate, anti–programmed cell death 1 (PD-1) antibody, and chimeric antigen receptor (CAR) T cells.

In order to understand the mechanism by which IA NEO100 enables transient opening of the BBB, we examined the 2 main methods for BBB transport: (i) transcellular transport, which involves passing across the endothelial cells (ECs), and (ii) paracellular transport, which involves passing through the intercellular space between the ECs, and it is mainly regulated by the presence of junctional complexes between adjacent ECs, consisting of tight junctions and adherent junctions. Tight junctions are connected areas in the upper part of the apical section of the plasma membrane that stitch ECs together, constituting the first and main seal that regulates the paracellular transport between cells.[2] The amphipathic properties of NEO100 led us to hypothesize that the molecule could intercalate between the phospholipids within the plasma membranes of the ECs, which would directly enhance the transcellular transport pathway. Additionally, subsequent increase in membrane fluidity would translate into a transient tight junction protein translocation from the cellular membrane to the cytoplasm, thereby enhancing the paracellular diffusion across the BBB. We propose that NEO100 could be applied intra-arterially in the clinic to immediately and transiently open the BBB, facilitating the transportation of therapeutics across the BBB with minimal effects on normal brain function.

Methods

Primary Cultures and Cells

Human tissues were obtained following written informed consent from patients in accordance with the Declaration of Helsinki guidelines and the institutional review board (HS-09-00520) at Keck School of Medicine, USC. Data regarding cell lines and culture are included in Supplementary Methods.

Cellular Barrier Disruption

For transepithelial experiments, 1.5×10^5 Madin-Darby Canine Kidney (MDCK1) cells were seeded on 12-well 0.4 μm pore-size Transwell inserts. For transendothelial experiments, inserts were previously coated with Matrigel. Primary cultures of astrocytes (1.5×10^5/well) were cultured on the bottom of the inserts and 1.5×10^5 primary brain ECs were seeded on top. Once confluent, cells were treated with NEO100 for different times, then a fluorescein isothiocyanate (FITC) antibody was added to the top chamber and cells were incubated for 2 h at 37 °C. Medium from the upper and

lower chambers was read in a FLUOstar Omega microplate reader. Transepithelial/transendothelial electrical resistance (TEER) was studied using a Millicell ERS-2 Volt/Ohm meter (Millipore).[9] Background resistance obtained in the wells without cells (80–100 Ω/cm^2) was subtracted.

Plasma Membrane Permeabilization

To study the effects of NEO100 on plasma membrane permeability, a ReadyProbes Cell Viability Imaging Kit was used, consisting of a blue fluorescent probe that stained all cells and a green fluorescent probe that stained the nuclei of cells with compromised plasma membranes. Cultured overnight were 2 × 10^4 brain ECs treated with 1 mM NEO100 for the indicated times. Brain ECs were imaged with an EclipseTE300 Inverted Microscope (Nikon).

Western Blot

Membrane and cytosolic proteins were extracted with a Mem-PER Plus Membrane Protein Extraction Kit (ThermoFisher Scientific).[10] Proteins were separated by sodium dodecyl sulfate–polyacrylamide gel electrophoresis and transferred to nitrocellulose membranes. Primary antibodies used were rabbit anti–claudin-3 (ab15102), rabbit anti–claudin-5 (ab15106), rabbit anti-JAM (junction adhesion molecule; ab125886), rabbit anti–ZO-1 (zonula occludens 1; ab216880) (1:500, Abcam), rabbit anti-occludin (1:200, Abcam, ab222691), rabbit anti-CD31 (1:1000, Cell Signaling Technology, #77699), and mouse anti–β-actin (1:1000, Proteintech #66009). Secondary antibodies used were horseradish peroxidase–conjugated goat anti-mouse (1:2500, Proteintech, SA00001) and goat anti-rabbit (1:2500, Cell SignalingTechnology, #7074).

Transmission Electron Microscopy

Ultrathin sections of the brains previously processed with Pelco BioWave Pro were cut at 99 nm and collected on 200-mesh copper grids. The grids were post-stained in uranyl acetate (0.2%) and filtered for 15 min. Grids were further stained with lead citrate and filtered for 5 min. The Tecnai Spirit G2TEM (Nanoscience Initiative) with an installed MegaView camera was used to image the samples.

Immunostaining

The detailed protocol has been described.[11] Primary antibodies used were rabbit anti-human CD3 (Cell Signaling, 99940), rabbit anti-CD8 (Abcam, ab4055), FITC-conjugated Armenian hamster anti-mouse PD-1 (ThermoFisher Scientific, 11-9985-82), and rat anti-mouse PD-1 (Bio X Cell, BE0146). The secondary antibody was Alexa Fluor 647 goat anti-rabbit (Abcam, ab150083). Pictures were taken in a Zeiss LSM 510 confocal microscope. Due to the short wavelengths (excitation wavelength = 367 nm and emission wavelength = 463 nm), a 2-photon laser was used for methotrexate. DAPI (4′,6-diamidino-2-phenylindole) or propidium iodide was used to stain cell nuclei.

In Vivo Studies

All animal protocols were approved by USC's Institutional Animal Care and Use Committee, and strictly adhered to. We acquired 6- to 8-week-old immunocompetent male/female C57BL/6 and BALB/c mice from the Jackson Laboratory. To evaluate IA NEO100–induced anti–PD-1 antibody brain entry, an intracranial syngeneic mouse glioma was established by implanting GL261 (1 × 10^4) mouse glioma cells intracranially in immunocompetent C57BL/6 mice. For the demonstration of humanized CD3+ CAR T cells (Kind gift from Alan Epstein's lab, USC) brain entry, primary CNS lymphoma xenografts were established by inoculating Raji B-cell lymphoma (5 × 10^5 cells, Raji/Luc–green fluorescent protein (GFP) intracranially into nonobese diabetic severe combined immunodeficient (NOD/SCID) interleukin (IL)-2 receptor-gamma^{null} mice. To avoid false positives, the experimental animals were perfused with 0.9% normal saline solution before euthanasia. The detailed procedures of ultrasound-guided intracardiac injection and IA catheter placement are described in Supplementary Methods.

Statistics

Statistical analyses were performed using GraphPad Prism 7.0. $P < 0.05$ was considered significant. A two-tailed *t*-test or 1-way ANOVA followed by Dunnett's orTukey's multiple comparison tests were used. For primary cultures, each patient-derived sample was considered the unit of analysis and accounted for an independent *n*-value, assayed in triplicate. At least 3 different patient-derived samples were used per experiment. For in vivo studies, $n = 3$ per condition.

Data regarding chemical and high performance liquid chromatography (HPLC) analysis, as well as supporting methods, can be found in the Supplementary Material.

Results

NEO100 Enhances Barrier Permeability at Subcytotoxic Doses

To study the in vivo effects of NEO100 on barrier permeability, we used an MDCK1 cell monolayer[12] as a classic model of the cellular transport barrier, and primary brain ECs with normal human astrocytes as a specific model of the BBB. The diffusion of an FITC-labeled antibody across Transwell inserts was measured at different NEO100 concentrations. The integrity of the MDCK1 barrier was significantly affected at 2 mM NEO100, while the brain ECs + astrocyte barrier was disrupted at 1 mM NEO100 (Figure 1A), both subcytotoxic concentrations (Supplementary Figure 2). Using TEER measurements, we observed that the barriers were significantly disrupted 10 min after NEO100 administration and remained opened during the 3 h treatment (Figure 1B), but fully recovered 18 h after removal of the compound (Figure 1C). These effects were not retained when NEO100 was conjugated to TMZ (Supplementary Figure 3).

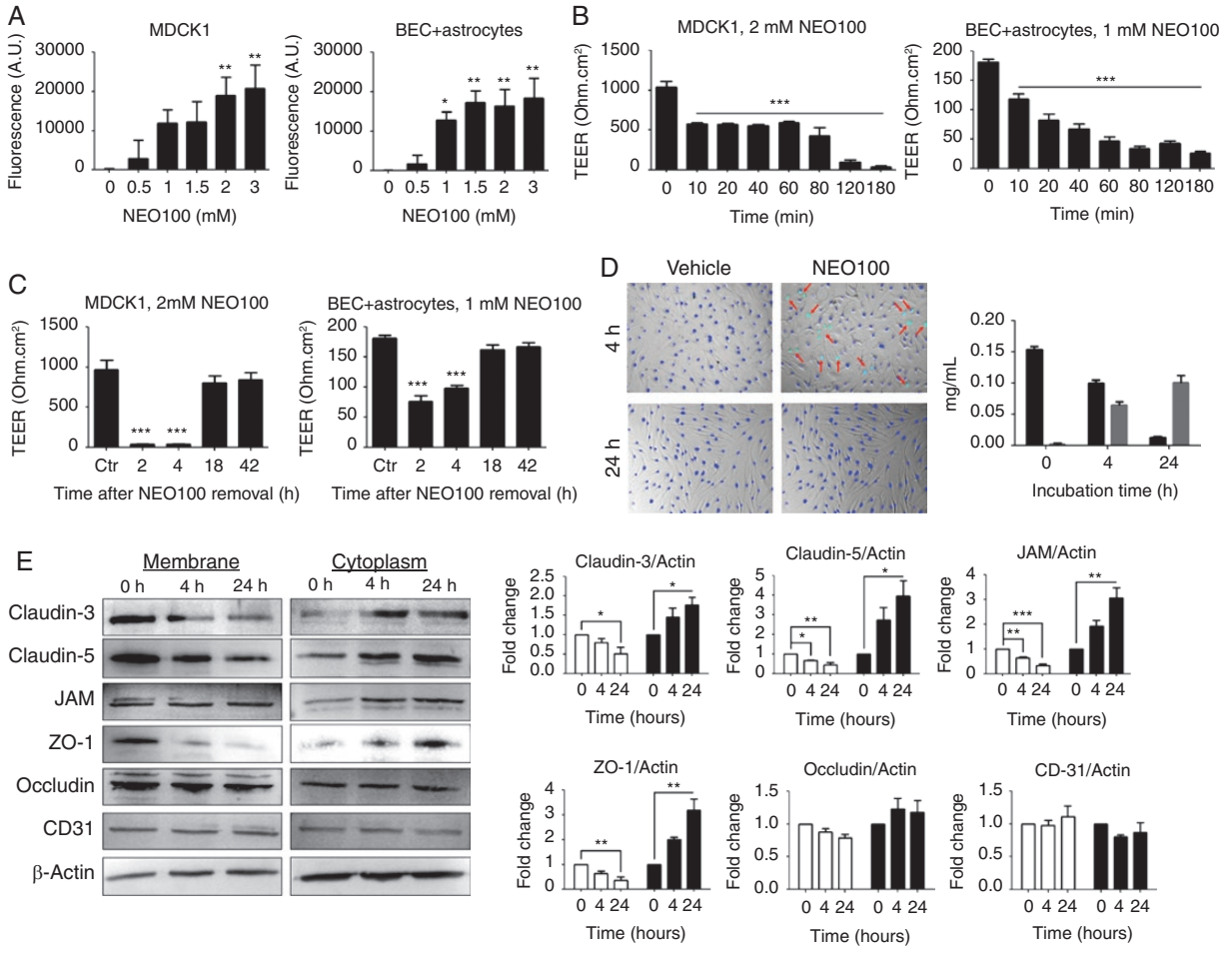

Fig. 1 NEO100 increases cell barrier permeability. (A) The permeability of MDCK1 and patient-derived brain ECs (BEC) + astrocyte barriers at different NEO100 concentrations for 4 h was determined measuring the diffusion of an FITC-conjugated antibody across 0.4 μm pore-size Transwell inserts after 2 h at 37 °C. *$P < 0.05$; **$P < 0.01$ (relative to vehicle-treated cells). (B) The changes of permeability with time upon treatment with NEO100 at 2 mM (MDCK1, left) or 1 mM (BEC + astrocytes, right) were studied with a TEER ohmmeter. ***$P < 0.001$ (relative to vehicle-treated cells). (C) After a 3-h treatment with 2 mM NEO100 (MDCK1, left) or 1 mM NEO100 (BEC + astrocytes, right), NEO100 was removed and the recovery of the membranes was determined with a TEER ohmmeter. ***$P < 0.001$ (relative to vehicle-treated cells). (D) BECs were treated with vehicle or 1 mM NEO100 for the indicated times. NucBlue (blue) was used to stain all cell nuclei, and NucGreen (green) was used to stain the nuclei of BECs with compromised plasma membranes (red arrows). The bar graph shows the concentration of NEO100 and its stable metabolite perillic acid remaining in the BEC supernatants after the indicated timepoints, measured by HPLC. (E) BECs were treated for 4 h or for 24 h with vehicle or 1 mM NEO100. Representative western blots showing the levels of the tight junction (TJ) or accessory proteins claudin-3, claudin-5, JAM (upper band seen in western blot), ZO-1 and occludin in the membrane or cytoplasmic fractions. CD31 was included as a control of non-TJ membrane protein. β-actin was used as a loading control. The bar graphs represent the average pixel density recorded by ImageJ of 3 independent western blots. *$P < 0.05$; **$P < 0.01$, ***$P < 0.001$ (relative to vehicle-treated cells).

To study the mechanism of NEO100-mediated permeabilization via the transcellular pathway,[13] we used a blue fluorescent probe that stains all brain EC nuclei, and a green fluorescent probe, which stains only the nuclei of cells whose membrane integrity is compromised. Treatment with 1 mM NEO100 for 0.5 h caused brain EC membrane permeabilization, an effect observed for up to 6 h, with the highest number of cells permeabilized after 4 h (Figure 1D, Supplementary Figure 4). However, after 24 h of continuous treatment with NEO100, the integrity of the membrane was reestablished. HPLC analysis of the supernatants of brain ECs treated with NEO100 showed that, while 65% of NEO100 was found after 4 h, only 8% of NEO100 remained in the supernatants after 24 h of incubation. Correspondingly, the levels of perillic acid, the stable metabolite of NEO100,[14] increased with time, indicating that NEO100 was being partially metabolized (Figure 1D, Supplementary Figures 4, 5).

We then examined the effects of NEO100 treatment on the paracellular pathway, a passive diffusion process through the junctional complexes between brain ECs.[15] We treated cells with vehicle or 1 mM NEO100 for 4 h and extracted the integral membrane proteins and membrane-associated proteins separately from

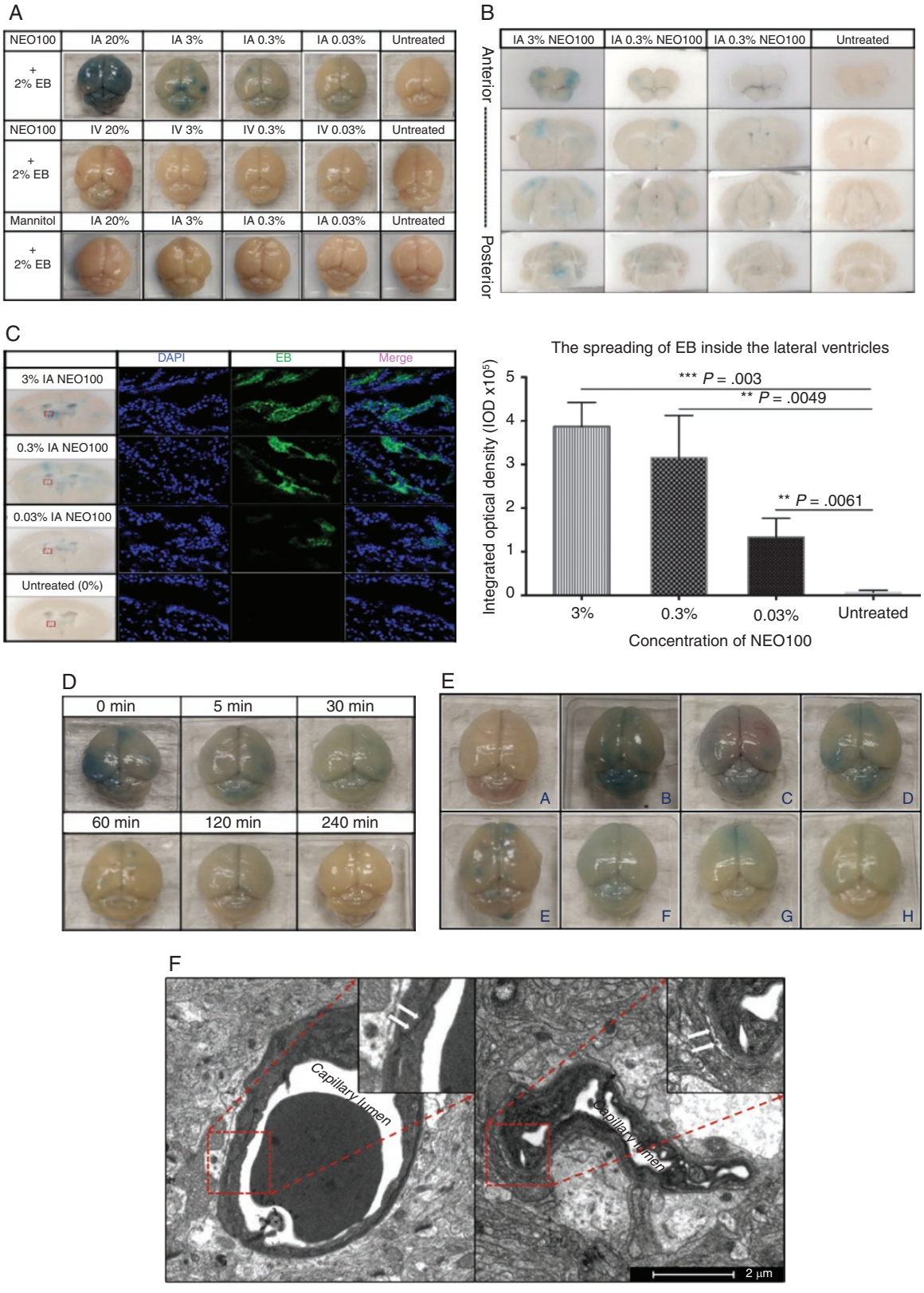

Fig. 2 IA NEO100 causes an immediate, transient, and reversible BBB disruption in vivo. (A) Representative pictures of brains from mice treated with different concentrations of IA NEO100 (upper), i.v. NEO100 (middle), or IA mannitol (lower). Neither i.v. NEO100 nor IA mannitol led to

the soluble cytoplasmic proteins. NEO100 increased the levels of tight junction and cytoplasmic accessory proteins in the cytoplasmic fraction, decreasing their membrane levels (Figure 1E). Comparable results were obtained in vivo using confocal microscopy (Supplementary Figure 6). No changes were observed in CD31, which is localized at intercellular junctions and contributes to the maintenance of barrier integrity but is not a tight junction protein[16] (Figure 1E). These effects disappeared after removal of NEO100 (Supplementary Figure 7), indicating that the delocalization of the tight junctions and cytoplasmic accessory proteins from the cell membrane to the cytoplasm is temporary and reversible.

Treatment of brain ECs with 1 mM NEO100 for 24 h (when the highest differences in tight junction protein localization were observed) did not cause an overall downregulation of the tight junctions compared with vehicle (dimethyl sulfoxide)-treated cells, as evidenced by the mRNA expression levels of 84 genes encoding tight junction proteins (Supplementary Figure 8). This indicates that the barrier permeabilization effects of NEO100 take place at the protein localization level.

IA NEO100 induces in vivo BBB opening

Due to the limitations of surgical field exposure under microscope for carotid catheter placement in mice, the IA NEO100 infusion was simulated using an ultrasound-guided intracardiac injection, delivering NEO100 directly into the intracranial arteries from the left ventricle of the heart (Supplementary Figure 12). IA NEO100 led to BBB opening in a dose-dependent manner, as evidenced by the higher amounts of extravasated Evan's blue (EB; 961 Da) obtained with higher NEO100 doses (Figure 2A–C). However, when NEO100 was administered i.v., no BBB breaching was observed. Similar results were obtained when EB was replaced by an FITC-conjugated cytochrome *C* or a rabbit anti-mouse immunoglobulin (Ig)G antibody (Supplementary Figures 10, 11). In contrast, replacing NEO100 with mannitol led to no extravasated EB (Figure 2A).

To study the kinetics of the IA NEO100-induced BBB opening, IA 3% NEO100 was followed by i.v. 2% EB given after the indicated different timepoints. IA NEO100 caused an immediate BBB opening, which lasted between 2 and 4 h (Figure 2D). These results indicate that IA NEO100 mediates a transient and reversible BBB opening, with the integrity of BBB being fully recovered 4 h after NEO100 administration. We next determined the time needed for the brain to clear up the extravasated EB. Immediately after IA 3% NEO100 was administered, 2% EB was given i.v., and the perfused brain tissues were collected after different timepoints (30 min, 120 min, 240 min, 1 day, 3 days, 5 days, and 7 days). Once the EB had spread within the brain, it remained for up to 7 days after BBB disruption was reverted (Figure 2E).

Transmission electron microscopy imaging of the ultrastructure changes in tight junctions around the lumen of cerebral vessels showed a tight continuous line between ECs in the normal tissue, which was replaced by broken and open spaces between the ECs in IA 0.3% NEO100-treated mice (Figure 2F), the concentration that was selected for further studies involving intracardiac injections. These results confirmed our in vitro data (Figure 1), suggesting that disruption of cell-cell contacts contributes to the IA NEO100-mediated BBB opening.

Currently, the disruption of BBB via rapid infusion of a hyperosmolar mannitol solution via IA catheter represents the main clinical method to enhance the transport of substances into the brain parenchyma.[2] However, administering mannitol via ultrasound-guided intracardiac injection led to no extravasated EB (Figure 2A), which could be due to a loss of its hyperosmotic properties with intracardiac injection. To better compare the levels of BBB breaching while ensuring the preservation of the hyperosmotic properties of mannitol, we used the standard osmotic delivery via IA catheter placement through the common carotid artery to deliver NEO100 and mannitol. Increasing volumes (40, 150, and 450 μL) of 25% mannitol were compared with 40 μL 3% NEO100, both administered via IA catheter placement in the common carotid artery. Not even the highest volume (450 μL) of hyperosmotic 25% mannitol induced a BBB disruption as strong as the one obtained with 40 μL 3% NEO100, as evidenced by the significantly higher EB spreading within the brains upon NEO100 treatment. Furthermore, while mannitol-mediated EB spreading was limited to the brain hemisphere where it was delivered, NEO100-mediated EB spreading reached virtually all areas of the brain (Figure 3).

IA NEO100 facilitates brain entry of the non-BBB-permeable small molecule therapeutic methotrexate

We next evaluated the potential of IA NEO100 (accomplished by intracardiac injection) to mediate the brain penetration of small-molecule therapeutics whose entry is usually impeded by the BBB. Methotrexate (454 Da) is a chemotherapy whose clinical efficacy in CNS lymphoma is limited due to poor drug penetration across the BBB.[17] Administration of high doses of methotrexate is therefore

detectable extravasated EB, while IA NEO100 caused a dose-dependent BBB breaching and, consequently, EB spreading. (B) Coronal sections (from anterior to posterior) from the mice treated with decreasing doses of IA NEO100 (3%, 0.3%, 0.03%, and 0%). (C) The autofluorescence of EB was captured around ventricle areas and quantified. IA NEO100 led to a dose-dependent significantly higher EB penetration into the brains, compared with untreated mice. (D) Two percent EB was given i.v. via the tail vein at the indicated timepoints after IA 3% NEO100 was administered. Two hours after the procedures, mice were perfused upon euthanasia and brains were collected. (E). Representative pictures of (i) normal mouse brains, and brains at different timepoints ([ii] 30 min, C-120 min, D-240 min, E-1-day, F-3 days, G-5 days, and H-7 days) post IA 3% NEO100 + i.v. 2% EB simultaneous application. (F) Transmission electronic microscopy (TEM) pictures showing changes in the ultrastructure of the BBB. A tight solid continuous line between the ECs in the normal brain (left) was replaced by broken and open spaces in IA NEO100-treated brain (right).

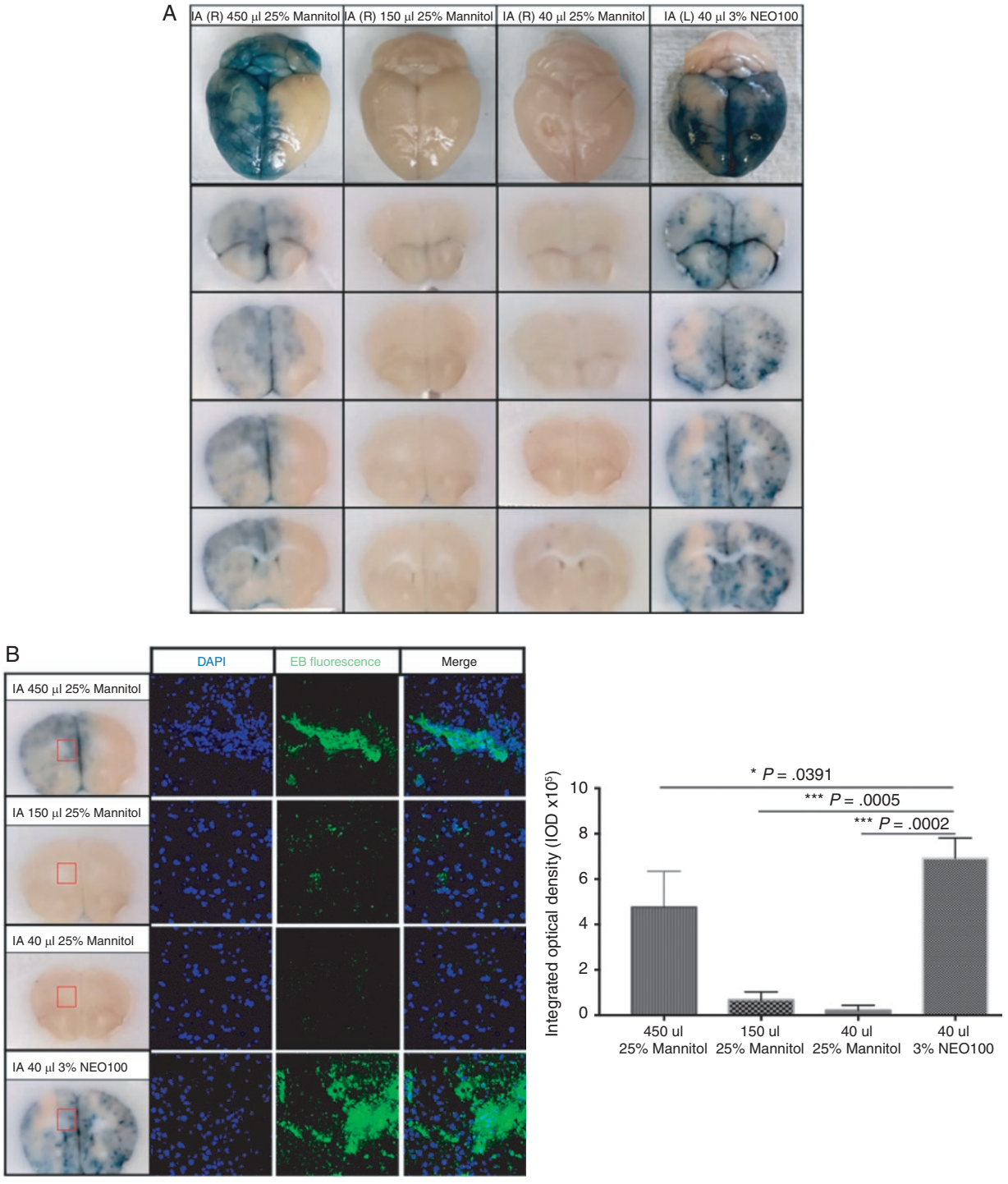

Fig. 3 NEO100 causes a stronger BBB disruption than hyperosmotic mannitol when administered via IA catheter placement through common carotid artery. (A) The extravasated EB could be visualized in brains treated with 40 µL IA 3% NEO100, whereas IA 25% mannitol did not induce BBB disruption unless the injected volume was escalated to 450 µL. Furthermore, while mannitol-mediated EB spreading was limited to the brain hemisphere where it was delivered (R-right), NEO100-mediated EB spreading (delivered to the L-left hemisphere) reached virtually all over the brain. (B) The autofluorescence of EB was captured by confocal imaging and quantified. 40 µL IA 3% NEO100 led to significantly higher EB penetration, compared with different volumes of IA 25% mannitol.

required to achieve therapeutic concentrations in the CNS, which results in increased systemic and neurological toxicity.[18]

To prove the potential of IA NEO100-induced efficient methotrexate brain entry, the experimental animals were treated for 2 h with IA NEO100 alone, i.v. methotrexate alone, or IA NEO100 + i.v. methotrexate; and the autofluorescence emitted by methotrexate in the perfused brains was detected by a 2-photon laser. Methotrexate spreading inside the brains was significantly higher in IA NEO100 + i.v. methotrexate-treated animals (Figure 4A). Accordingly, the amount of methotrexate detected using HPLC in the brain parenchyma and CSF was significantly higher in IA NEO100 + i.v. methotrexate-treated animals (Figure 4B).

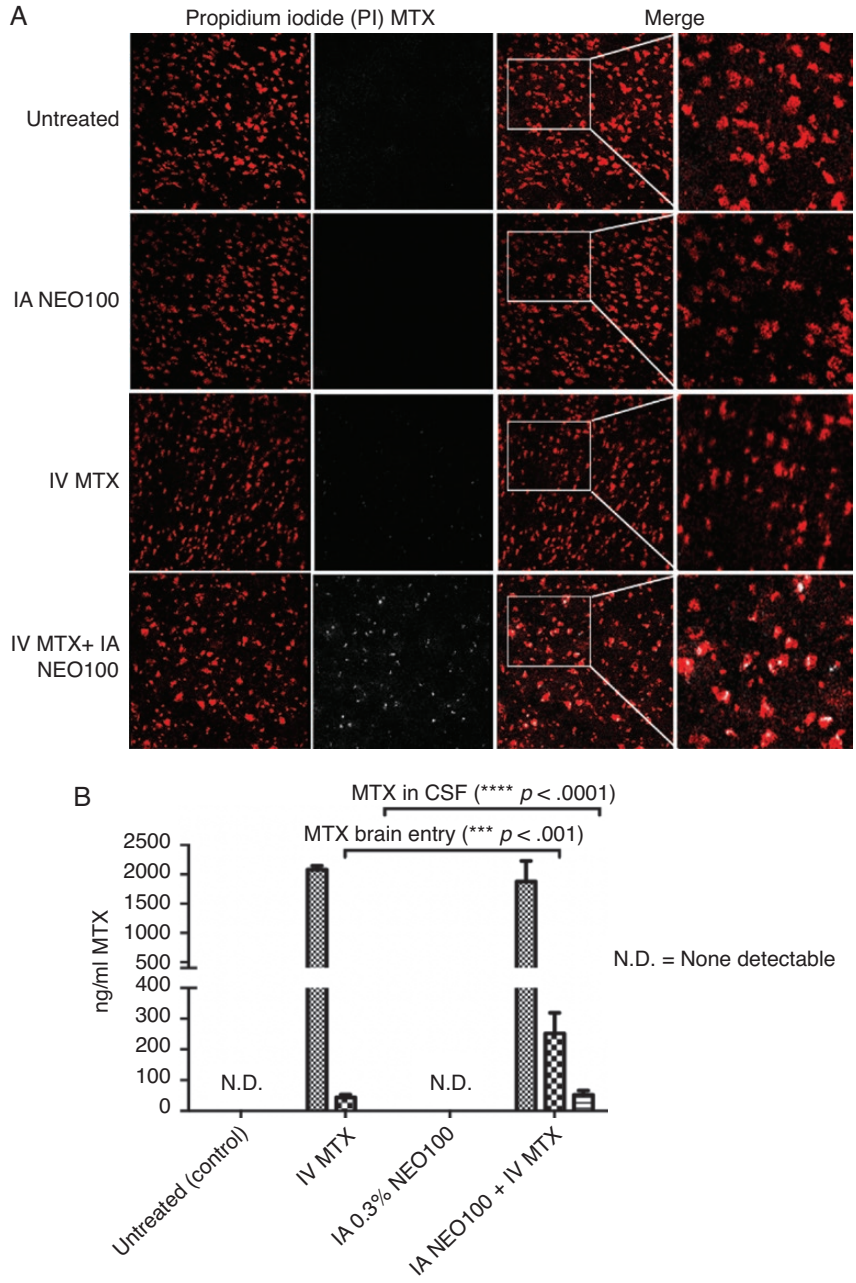

Fig. 4 IA NEO100 facilitates brain delivery of the non-BBB-permeable small molecule therapeutic methotrexate (MTX). (A) The autofluorescence of MTX was detected using 2-photon microscopy. Propidium iodide (red) was used to stain cell nuclei. The extravasated MTX (white) was detected in brains from mice treated with IA 0.3% NEO100 + i.v. MTX, but not in control mice or in mice treated with IA 0.3% NEO100 alone, while some sporadic MTX was detected in mice treated with i.v. MTX alone. (B) MTX levels in the serum, brain, and CSF were measured by HPLC. IA 0.3% NEO100 significantly enhanced MTX penetration into the brains and CSF compared with i.v. MTX (1.2 mg/kg) alone.

NEO100-mediated BBB opening facilitates brain entry of the therapeutic antibody anti–PD-1

We wanted to determine whether IA NEO100 could enhance brain delivery of large IgG therapeutics while keeping their pharmacological properties intact. The interaction of PD-1 receptor on T cells with its ligand, PD-L1, on the tumor cells reduces T-cell signaling function, resulting in a depletion of CD8+ cells inside tumors. The use of inhibitors that block the PD-L1/PD-1 interaction can prevent the cancer from evading the immune system.[19] We first determined whether NEO100 could facilitate the entry of an FITC-labeled anti-mouse PD-1 antibody into intracranial tumors. As shown in Figure 5A, IA 0.3% NEO100 significantly enhanced anti–PD-1 penetration into the brain tumor compared with untreated and i.v. FITC/anti–PD-1, *with highly preferential accumulation in the tumor tissue but not in normal brain*.

We next studied whether IA NEO100 administration could affect the efficacy of the checkpoint inhibitor anti–PD-1 antibody in blocking PD-1 pathway and repopulate the exhausted CD8+ T-cell population. Following i.v. administration of an unlabeled anti-mouse PD-1 antibody (1 mg/kg) with or without IA 0.3% NEO100 to immunocompetent mice bearing syngeneic mouse glioma (1×10^4 GL261 cells injected intracranially into C57BL/6 mice 3 wk ago), we detected the CD8+ T lymphocyte spreading inside the tumor by immunohistochemistry using both fluorescent and biotinylated antibodies (Figure 5B). IA 0.3% NEO100 significantly boosted the CD8+ T-cell population in the glioma tumors, compared with untreated mice and mice treated with i.v. anti–PD-1 (1 mg/kg) alone. These data suggest that IA NEO100 not only increases the antibody penetration into the tumor tissues, but also restores immune function in the tumor microenvironment via the anti–PD-1 antibody.

IA NEO100 enhances CAR T-cell brain tumor penetration in vivo

CAR T cells provide a new strategy to bypass the defective immune system for cancer treatment. However, poor CAR T-cell trafficking to the brain tumor due to the cells' inability to cross the BBB is still a major limitation for the effectiveness of this approach.[20] To test whether IA NEO100-induced BBB opening could be applied to the delivery of CAR T cells, an intracranial primary CNS lymphoma xenograft was established in NOD/SCID IL-2 receptor gamma^{null} mice (5×10^5 human B-cell Raji/Luc-GFP lymphoma cells were injected intracranially). Upon confirmation of tumor uptake, mice were treated with i.v. CAR T cells (5×10^6) alone or with IA 0.3% NEO100 + i.v. CAR T cells (5×10^6). Immunostaining with biotinylated and fluorescent antibodies was performed to identify the spreading of CD3+ cells within tumor tissues. Untreated animals served as a negative control, while CD3+ cells from cultures of Lym-1 CAR T cells served as positive control. IA 0.3% NEO100 significantly increased the population of CD3+ CAR T cells *highly preferentially accumulated* within the tumors compared with untreated mice and with mice treated with i.v. CAR T cells alone, *but not in normal brain* (Figure 6A).

Discussion

The maintenance of BBB integrity is essential for CNS homeostasis, but it hinders the delivery of therapeutics for many neurological disorders. IA mannitol remains the gold standard for transient BBB disruption. However, limited clinical data and high variability in the degree of BBB disruption obtained, with subsequent fluctuating concentrations of drugs in the CSF,[21,22] limit its applications in the clinical setting. Thus, novel mechanisms that allow a safe and transitory opening of the BBB without permanently affecting the integrity of the barrier are badly needed.

Here, we demonstrate that IA NEO100 transiently and reversibly permeabilizes the BBB at subcytotoxic doses (Figures 1–3, Supplementary Figure 2). In vitro studies with cellular barriers showed that NEO100 affects the passive transcellular pathway, transiently permeabilizing the membranes of patient-derived brain ECs (Figure 1, Supplementary Figures 4, 5). In addition, NEO100 acts on the paracellular pathway, by reversibly delocalizing the tight junction proteins from the brain EC membrane toward their cytoplasm (Figures 1, 2, Supplementary Figures 6, 7). These effects allow for a quick recovery of BBB integrity after removal or clearance of NEO100. Microarray analysis of 84 genes encoding tight junction proteins showed no significant change in their expression pattern upon treatment with NEO100 (Supplementary Figure 8), confirming that the observed effects are not due to changes in mRNA or protein production, but rather are at the protein localization level. Transmission electron microscopy images provided strong supporting in vivo evidence of altered ultrastructure of the tight junction between ECs in brain tissues from animals treated with IA NEO100 (Figure 2F), further confirming our in vitro results.

Our preliminary in vivo data showed that IA NEO100 causes an immediate, transitory, and reversible BBB opening. However, no BBB breaching was achieved when NEO100 was given by i.v. injection via the tail vein, likely due to NEO100 being metabolized or too diluted before reaching the cerebral arteries, compared with intracardiac injection. Similarly, mannitol was not able to mimic the BBB-opening activity of NEO100 when applied in the same (intracardiac) manner, indicating different mechanisms of action. This lack of BBB disruption could be due to a loss of its hyperosmotic properties with intracardiac injection due to a decrease of its concentration below the hyperosmolar levels required to obtain cell shrinkage that pulls apart the tight junctions between adjacent ECs in the cerebrovasculature.[22] To ensure the preservation of the hyperosmotic properties of mannitol, we used the standard osmotic delivery via IA catheter placement through the common carotid artery. Although some level of localized BBB breaching was obtained when mannitol was delivered via catheter, much lower volumes and concentrations of NEO100 led to a significantly higher BBB disruption and EB spreading within the brains (Figure 3). In summary, NEO100

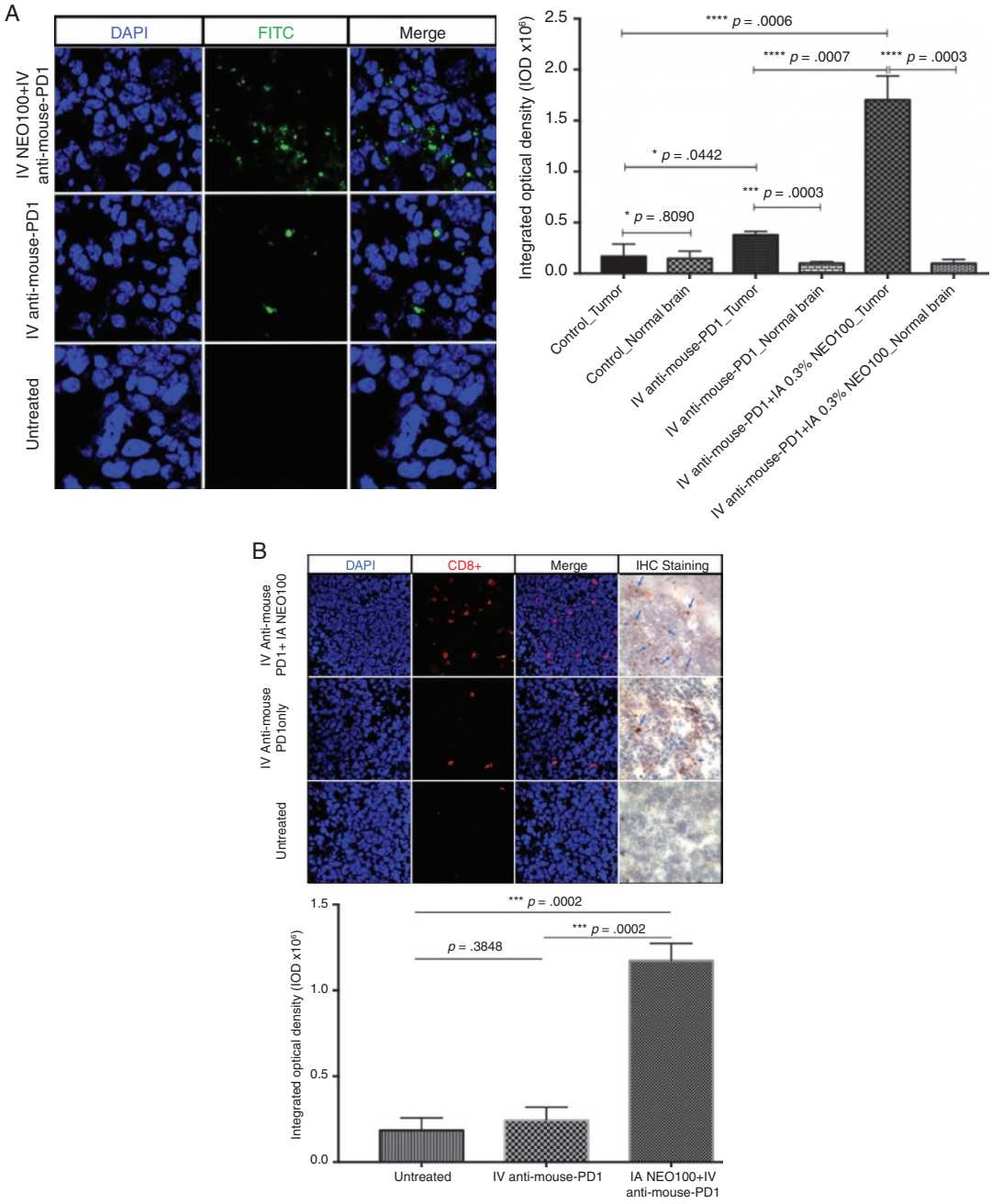

Fig. 5 IA NEO100 facilitates brain tumor entry of the checkpoint inhibitor anti–PD-1 antibody, enhancing its pharmacological properties. (A) IA 0.3% NEO100 significantly (***$P = 0.0007$) enhanced the brain tumor entry of an FITC-conjugated anti–PD-1 antibody (1 mg/kg) in mice bearing syngeneic glioma (3 wk after the intracranial implantation of 1×10^4 GL261 cells) but not in normal brain (***$P = 0.0003$), compared with mice treated with conventional i.v. infusion of FITC/anti–PD-1 alone. (B) Immunohistochemistry (IHC) and confocal images showing the replenishment of CD8+ T cells (red arrowheads) inside the brain tumors of mice bearing syngeneic glioma. The levels of CD8+ cells were significantly higher in IA 0.3% NEO100 + i.v. unlabeled anti–PD-1 treated mice compared with untreated mice or mice treated with i.v. diffusion of unlabeled anti–PD-1 alone.

induced an immediate, reversible, and much more efficient BBB opening than the gold standard mannitol. Rather than cellular shrinkage due to hyperosmolarity, we propose that the amphipathic properties of NEO100 cause a transient disruption of the paracellular and transcellular pathways, allowing for temporary transport of substances across the BBB. Since IA NEO100-mediated BBB disruption occurs in a time- and dose-dependent manner, the extent of BBB opening could be controlled by manipulating the volumes and concentrations of NEO100 applied.

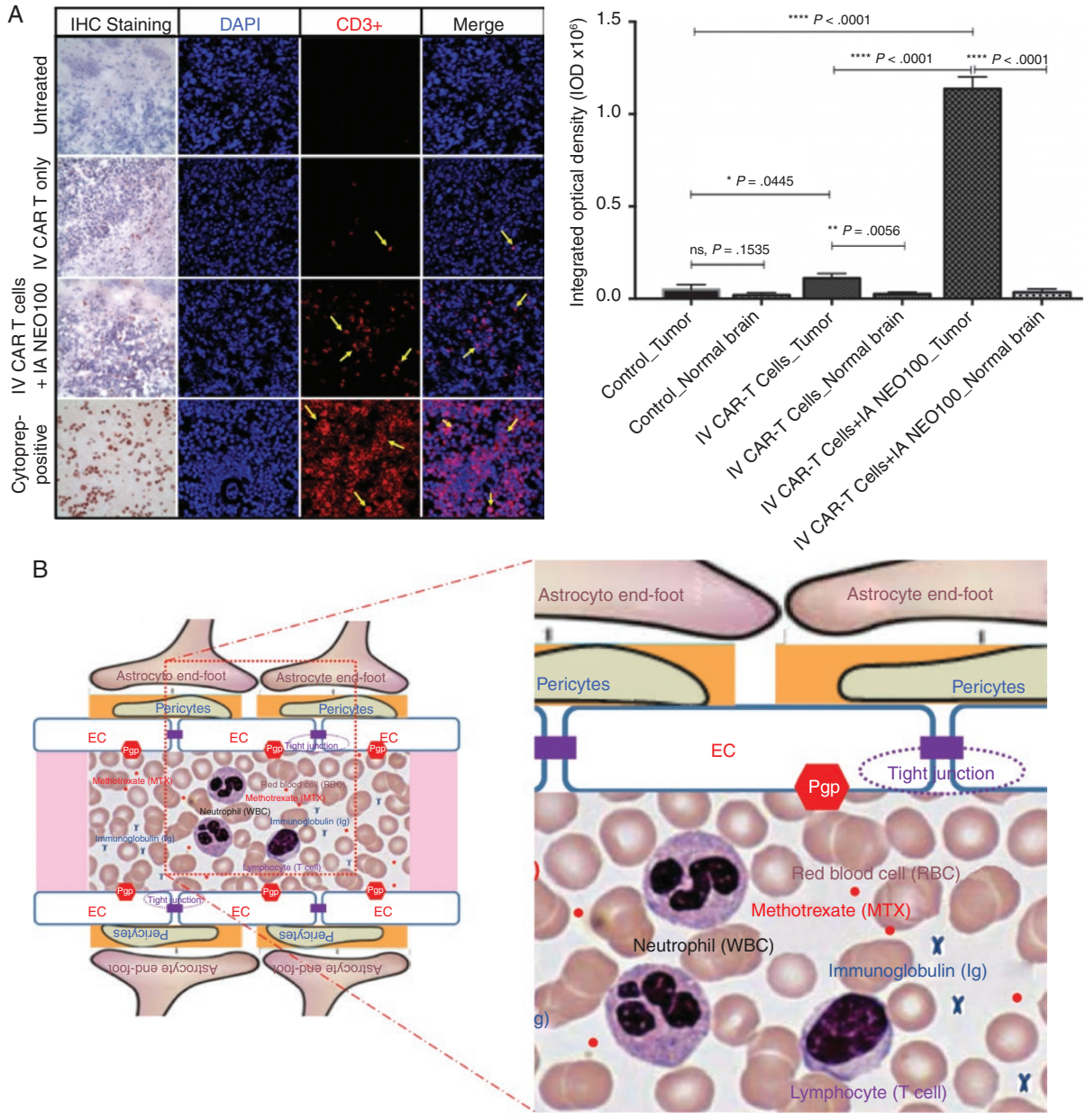

Fig. 6 IA NEO100 mediates human CAR T-cell penetration into brain tumors. (A) Immunostaining was performed to identify the spreading of CD3+ cells within tumor tissues harvested from the mice bearing intracranial human B-cell Raji CNS xenografts and treated with i.v. CAR-T (5×10^6) cells with or without IA 0.3% NEO100. Untreated animals served as a negative control, while CD3+ cells from cultures of Lym-1 CAR T cells served as positive control. IA NEO100 enabled highly preferential accumulation of CD 3+ Lym-1 CAR T cells in the lymphoma xenografts (****$P < 0.0001$), compared with untreated mice, or with mice treated with i.v. CAR T cells infusion alone. (B) Schematic representation showing the most relevant structural elements of the BBB, ie, ECs, pericytes, and astrocytic end-foot processes, and the relative size of, immunoglobins, white blood cells (neutrophils, 10–12 μm in diameter; and lymphocytes, 6–14 μm in diameter), and red blood cells (7.5 μm in diameter).

Our results showing effective brain entry and preferential tumor localization of PD-1 antibodies and CAR T cells were achieved at fairly low concentrations of IA NEO100 (0.3%). It is noteworthy that these concentrations did not result in any obvious side effects. The treated animals recovered from surgery and continued to thrive in the absence of noticeable signs of toxicity. While this outcome suggests a good safety profile, more detailed in vivo studies are needed for validation, including the application of this procedure in a larger animal model. For future clinical implementation in patients, IA injections of NEO100 are envisioned to be

performed via cannulation of the femoral artery with selective threading to the intracranial arteries (performed by interventional neuroradiology), representing a human equivalent to intracardiac injections in mice. This approach represents a routine procedure that is commonly performed by endovascular neurosurgeons in the clinic in the context of cerebral angiograms, aneurysm coiling, tumor embolization, and thrombectomies. Thus, the technique of reaching the base of the brain for injectates is well established, but repurposing it for BBB opening with NEO100 will require safety studies in phase I clinical trials.

Although the duration of BBB opening is fairly short, it suffices for pronounced brain entry of EB (Figure 3), methotrexate (Figure 4), PD-1 antibodies (Figure 5), and CAR T cells in the brain. In the case of the latter 2, we could further establish highly preferential accumulation in brain tumor tissue over normal brain tissue, which bodes well for therapeutic considerations. While our study did not investigate details of influx/efflux kinetics, we surmise that accumulation of PD-1 antibodies and CAR T cells within tumor tissue might be reinforced by the presence of tumor-specific targets, which presumably are absent in normal brain tissue. Furthermore, it is conceivable that the blood–tumor barrier within tumors, which generally already exists in a partially compromised state, is opened in a more substantial fashion by NEO100 than the BBB within normal brain tissue. While these details remain to be established, tumor-specific accumulation of PD-1 and CAR T cells, as evidenced by our results, represents a highly promising basis for future applications.

In the present studies, we have applied IA NEO100 delivery to an array of non-BBB-permeable therapeutic agents, from the small-molecule methotrexate to antibodies (anti–PD-1) and even CAR T cells (Figures 4–6, Supplementary Figures 10, 11). Regardless of the molecular size (relative sizes shown in Figure 6B) or physicochemical properties, IA NEO100 facilitated the brain entry of all therapeutics tested. IA NEO100-mediated anti–PD-1 delivery showed that IA NEO100 not only facilitates the brain entry physically, but also enhances its pharmacological properties, leading to a stronger replenishment of CD8+ cells inside the tumors (Figure 5). Moreover, IA NEO100-mediated BBB opening facilitated the transport of CD3+ CAR T cells into brain tumors, while only a few sporadic CD3+ cells were observed inside the tumor when CAR T cells were delivered by conventional i.v. infusion (Figure 6). Nowadays, standard i.v. infusion of CAR T cells is not enough to congregate these cells locally in the brain. Rather, i.v. delivery supports widespread systemic distribution, causing CAR T cells to get physically stuck in the lungs for several hours, then migrate to the liver, spleen, and lymph nodes, which augments the side effects of CAR T-cell therapy.[20,23] IA NEO100-facilitated transport of CAR T cells could have a revolutionary impact in CAR T-cell immunotherapy in glioblastoma and other malignant brain tumors.

In summary, we have shown that IA NEO100-mediated BBB opening represents an immediate, transient, reversible, and safe fashion to allow for optimal brain entry of therapeutic agents into the CNS, from small molecules to antibodies and even to CAR T cells. Specific pharmacokinetic studies would need to be carried out for each therapeutic agent, to optimize the dosage for maximum efficacy with minimum side effects. Although our studies were performed in mice with intracardiac injections to simulate IA delivery, we will be performing larger animal studies to simulate transfemoral delivery in humans. These animal models will be chosen on the basis of whether they have a *rete mirabile*, a plexus of small vessels in the base of the brain, which makes simulation of the human intracerebral vasculature extremely difficult. Therefore, large animal models (ie, rabbits that do not have a rete mirabile) will be performed in the future with transfemoral catheterization and delivery. Future validation of transfemoral NEO100 delivery in human clinical trials will hopefully validate IA NEO100 as tomorrow's clinical standard to facilitate the transport of CNS-targeted non-BBB-permeable medications, enabling superior therapeutic efficacy with minimal doses and side effects.

Supplementary Material

Supplementary data are available at *Neuro-Oncology* online.

Keywords

perillyl alcohol (POH) | NEO100 | blood-brain barrier (BBB) | drug transport | tight junctions

Funding

This work was supported by NeOnc Technologies, Inc (T.C.C.), the USC Wright Foundation (W.W.), the National Cancer Institute/NIH award 1R41CA217551 (W.W., T.C.C.), METAvivor Research and Support, Inc (A.H.S. and T.C.C.), and the Sharyl and Oscar Garza Research Fund (T.C.C.).

Conflict of interest statement. T.C.C. is the founder and stakeholder of NeOnc Technologies (Los Angeles, California). No potential conflict of interest was disclosed by the other authors.

References

1. Kaisar MA, Sajja RK, Prasad S, Abhyankar VV, Liles T, Cucullo L. New experimental models of the blood-brain barrier for CNS drug discovery. *Expert Opin Drug Discov.* 2017;12(1):89–103.
2. Hersh DS, Wadajkar AS, Roberts N, et al. Evolving drug delivery strategies to overcome the blood brain barrier. *Curr Pharm Des.* 2016;22(9):1177–1193.

3. Joshi S, Ergin A, Wang M, et al. Inconsistent blood brain barrier disruption by intraarterial mannitol in rabbits: implications for chemotherapy. *J Neurooncol.* 2011;104(1):11–19.
4. Marchi N, Angelov L, Masaryk T, et al. Seizure-promoting effect of blood-brain barrier disruption. *Epilepsia.* 2007;48(4):732–742.
5. Cho HY, Wang W, Jhaveri N, et al. Perillyl alcohol for the treatment of temozolomide-resistant gliomas. *Mol Cancer Ther.* 2012;11(11):2462–2472.
6. da Fonseca CO, Khandelia H, Salazar MD, Schönthal AH, Meireles OC, Quirico-Santos T. Perillyl alcohol: dynamic interactions with the lipid bilayer and implications for long-term inhalational chemotherapy for gliomas. *Surg Neurol Int.* 2016;7:1.
7. da Fonseca CO, Schwartsmann G, Fischer J, et al. Preliminary results from a phase I/II study of perillyl alcohol intranasal administration in adults with recurrent malignant gliomas. *Surg Neurol.* 2008;70(3):259–266;discussion 266–267.
8. Chen TC. "An open-label, phase 1/2A dose escalation study of safety and efficacy of NEO100 in recurrent grade IV glioma". *Safety and efficacy study in recurrent grade IV glioma.* 2016; https://clinicaltrials.gov/ct2/show/NCT02704858.
9. Srinivasan B, Kolli AR, Esch MB, Abaci HE, Shuler ML, Hickman JJ. TEER measurement techniques for in vitro barrier model systems. *J Lab Autom.* 2015;20(2):107–126.
10. Qoronfleh MW, Benton B, Ignacio R, Kaboord B. Selective enrichment of membrane proteins by partition phase separation for proteomic studies. *J Biomed Biotechnol.* 2003;2003(4):249–255.
11. Virrey JJ, Golden EB, Sivakumar W, et al. Glioma-associated endothelial cells are chemoresistant to temozolomide. *J Neurooncol.* 2009;95(1):13–22.
12. Cho MJ, Thompson DP, Cramer CT, Vidmar TJ, Scieszka JF. The Madin Darby canine kidney (MDCK) epithelial cell monolayer as a model cellular transport barrier. *Pharm Res.* 1989;6(1):71–77.
13. Tajes M, Ramos-Fernández E, Weng-Jiang X, et al. The blood-brain barrier: structure, function and therapeutic approaches to cross it. *Mol Membr Biol.* 2014;31(5):152–167.
14. Boon PJ, van der Boon D, Mulder GJ. Cytotoxicity and biotransformation of the anticancer drug perillyl alcohol in PC12 cells and in the rat. *Toxicol Appl Pharmacol.* 2000;167(1):55–62.
15. Engelhardt B, Sorokin L. The blood-brain and the blood-cerebrospinal fluid barriers: function and dysfunction. *Semin Immunopathol.* 2009;31(4):497–511.
16. Privratsky JR, Newman PJ. PECAM-1: regulator of endothelial junctional integrity. *Cell Tissue Res.* 2014;355(3):607–619.
17. Ferreri AJ, Crocchiolo R, Assanelli A, Govi S, Reni M. High-dose chemotherapy supported by autologous stem cell transplantation in patients with primary central nervous system lymphoma: facts and opinions. *Leuk Lymphoma.* 2008;49(11):2042–2047.
18. Hashemi-Sadraei N, Peereboom DM. Chemotherapy in newly diagnosed primary central nervous system lymphoma. *Ther Adv Med Oncol.* 2010;2(4):273–292.
19. Jiang X, Wang J, Deng X, et al. Role of the tumor microenvironment in PD-L1/PD-1-mediated tumor immune escape. *Mol Cancer.* 2019;18(1):10.
20. Migliorini D, Dietrich PY, Stupp R, Linette GP, Posey AD Jr, June CH. CAR T-cell therapies in glioblastoma: a first look. *Clin Cancer Res.* 2018;24(3):535–540.
21. Chu C, Jablonska A, Lesniak WG, et al. Optimization of osmotic blood-brain barrier opening to enable intravital microscopy studies on drug delivery in mouse cortex. *J Control Release.* 2019;317:312–321.
22. Doolittle ND, Miner ME, Hall WA, et al. Safety and efficacy of a multicenter study using intraarterial chemotherapy in conjunction with osmotic opening of the blood-brain barrier for the treatment of patients with malignant brain tumors. *Cancer.* 2000;88(3):637–647.
23. Visioni A, Kim M, Wilfong C, et al. Intra-arterial versus intravenous adoptive cell therapy in a mouse tumor model. *J Immunother.* 2018;41(7):313–318.